Estimation of Angular Spreads and Mean Angles of Arrival for Multiple Incoherently-Distributed Noncircular Sources

Sonia Ben Hassen
Electronic Systems and Communication Networks Engineering
Tunisia Polytechnic School
La Marsa, Tunisia
Email: sonia.benhassen@yahoo.fr

Faouzi Bellili, Abdelaziz Samet, and Sofiène Affes
INRS-EMT
Montreal, Qc, H5A 1K6, Canada
Email: bellili@emt.inrs.ca, samet@emt.inrs.ca, affes@emt.inrs.ca

Abstract—In this paper, we propose a new method for the estimation of the angular parameters (i.e., central DOAs and angular spreads) of noncircular and incoherently distributed (ID) signals. Contrarily to state-of-the-art techniques, the new method exploits the additional information about the angular parameters that is carried in the unconjugated covariance matrix. Contrarily to noncircular signals, this matrix is identically zero for the circular case and, therefore, it is totally ignored by all existing techniques when directly applied to noncircular sources thereby leading to performance degradations. It will be seen that the new method outperforms the main classical estimators that are all developed for circular sources only and that its performance advantage is more prominent at low SNR values and/or for low DOA separations.

Keywords—*Angular parameters estimation, multiple incoherently distributed sources, noncircularity of the signals.*

I. INTRODUCTION

Direction-of-arrival (DOA) estimation for multiple plane waves impinging on an arbitrary array of sensors has received much attention in array signal processing. Consequently, many DOA estimators have been studied, assuming different data models. Indeed, in a standard DOA estimation model, the signals are assumed to be generated from far-field point sources which travel along a single path to the antenna array. For this model, several methods have been studied in the literature [1]-[3]. However, in real surroundings, especially in modern wireless communication systems, local scattering in the source vicinity causes angular spreading. Therefore, the researchers considered a realistic signal model called spatially distributed source model. In the literature, distributed sources have been classified into two types: coherently distributed (CD) and incoherently distributed (ID) sources [4]. The assumption of uncorrelated ID sources has been shown to be relevant in wireless communications environments with a high base station. Therefore, many algorithms have been developed considering this assumption. Since for a distributed ID source, the components arriving from different directions are uncorrelated, then the rank of the noise-free covariance matrix in this case is different to the number of sources. Therefore, traditional subspace-based methods become not applicable. To deal with this problem, the researchers have defined the effective dimension of the signal subspace as the number of the first eigenvalues of the noise-free covariance matrix where most of the signal energy is concentrated.

They then proposed some subspace methods based on this pseudodecomposition [4, 5]. Later, authors proposed in [6, 7] more computationally attractive but less efficient methods based on the beamforming techniques. Furthermore, some other contributions [8, 9] have adopted the covariance fitting approach to estimate the angular parameters. Recently, authors proposed in [10] a robust version of the generalised Capon principle (GC) [7] which is the RGC method. This new method enables the estimation of the DOAs decoupled from that of the angular spreads of the sources. More recently, A. Zoubir *and al.* derived in [11] a new subspace-based algorithm for the estimation of the angular parameters of multiple ID sources. It uses the property of the inverse of the covariance matrix to exploit approximately the orthogonality between column vectors of the noise-free covariance matrix and the sample pseudonoise subspace. Then, it doesn't require the knowledge of the dimension of the signal subspace. Despite their efficiency, all the the aforementioned methods are developed only for circular sources.

Yet, noncircular complex signals are frequently encountered in digital communications [12]. Therefore, efforts have been directed to deriving new algorithms that exploit the unconjugated spatial covariance matrix for noncircular signals [12]-[14], but still for point sources. But to the best of our knowledge, no contributions have dealt so far with the problem of estimating the angular parameters assuming the signals to be generated from noncircular ID sources. Therefore, the aim of this work is to show the potential benefit of the noncircularity of the signals that could be gained in the angular parameters estimation for ID sources. In fact, we propose for the first time an algorithm that extends the recent method developed in [11] assuming circular ID signals to the case of noncircular ID signals.

This paper is organized as follows. In section II, we introduce the system model. In section III, we formulate the newly proposed algorithm. In section IV, some simulation results will be presented and some concluding remarks will be drawn out.

Throughout this paper, matrices and vectors are represented by bold upper case and bold lower case characters, respectively. Vectors are, by default, in column orientation, while $(.)^*$, $(.)^T$ and $(.)^H$ refer to conjugate, transpose and conjugate transpose, respectively. Moreover, E{.}, tr(.), $\|.\|_{\text{Fro}}$ and $\Re\{.\}$ stand for the expectation, trace, Frobenius norm and real part operators,

respectively. $\boldsymbol{I}_p$ and $\boldsymbol{0}_{p \times q}$ represent the $(p \times p)$ identity matrix and the $(p \times q)$ zero matrix, respectively. Finally, $\odot$ represents the Hadamard-Schur product operator.

II. System Model

Consider a uniform linear array of L identical sensors receiving the signals scattered from K distributed narrowband far-field sources. The output of the lth array sensor can then be modelled as a complex signal as follows:

$$x_l(t) = \sum_{k=1}^{K} \int_{-\pi/2}^{\pi/2} a_l(\theta) s_k(\theta, \boldsymbol{\psi}_k, t) d\theta + n_l(t), \quad (1)$$

where $a_l(\theta)$ is the response of the lth sensor to the unit energy source emitting from the direction θ and $s_k(\theta, \boldsymbol{\psi}_k, t)$ represents the complex angular signal distribution of the kth source that is parameterized by the unknown vector $\boldsymbol{\psi}_k = [\bar{\theta}_k, \sigma_k]^T$. $\bar{\theta}_k$ is the *central* DOA of the kth source defined as the mass center of the corresponding angular power density as follows:

$$\bar{\theta}_k = \int_{-\pi/2}^{\pi/2} \theta \rho_k(\theta, \boldsymbol{\psi}_k) d\theta, \quad (2)$$

with $\rho_k(\theta, \boldsymbol{\psi}_k)$ is its *normalized angular power density* satisfying:

$$\int_{-\pi/2}^{\pi/2} \rho_k(\theta, \boldsymbol{\psi}_k) d\theta = 1, \quad k = 1, 2, \ldots, K. \quad (3)$$

Moreover, σ_k is the angular spread of the kth source defined here as the standard deviation of angular deviation around the central DOA $\bar{\theta}_k$ of the kth scattered source. Finally, $n_l(t)$ represents the additive zero-mean spatially white noise at the lth sensor of the array.

Stacking the received data of the L sensors in a vector $\boldsymbol{x}(t) = [x_1(t), \ldots, x_L(t)]^T$, it follows from (1) that:

$$\boldsymbol{x}(t) = \sum_{k=1}^{K} \int_{-\pi/2}^{\pi/2} \boldsymbol{a}(\theta) s_k(\theta, \boldsymbol{\psi}_k, t) d\theta + \boldsymbol{n}(t), \quad (4)$$

where $\boldsymbol{a}(\theta) = [a_1(\theta), \ldots, a_L(\theta)]^T$ and $\boldsymbol{n}(t) = [n_1(t), \ldots, n_L(t)]^T$ are the array response, and noise vectors respectively. We also define the *conjugated* angular cross-correlation kernel of the kth and k'th sources arriving at the array with the directions θ and θ' as follows:

$$p_{kk'}(\theta, \theta'; \boldsymbol{\psi}_k, \boldsymbol{\psi}_{k'}) = \mathrm{E}\{s_k(\theta, \boldsymbol{\psi}_k, t) s_{k'}^*(\theta', \boldsymbol{\psi}_{k'}, t)\}. \quad (5)$$

We consider in this paper the ID source model. Then, for each source, the components arriving from different scatterers are uncorrelated. Moreover, we assume that all the distributed sources are mutually uncorrelated. Therefore, (5) can be written as:

$$p_{kk'}(\theta, \theta'; \boldsymbol{\psi}_k, \boldsymbol{\psi}_{k'}) = \sigma_{s_k}^2 \rho_k(\theta, \boldsymbol{\psi}_k) \delta(\theta - \theta') \delta_{kk'}, \quad (6)$$

where $\sigma_{s_k}^2$ is the power of the kth source, $\delta(\theta - \theta')$ is the Dirac delta-function and $\delta_{kk'}$ is the Kronecker delta. Furthermore, we assume that the sources are noncircular. Then, we define in the same way the *unconjugated* angular cross-correlation kernel as follows:

$$\begin{aligned} p'_{kk'}(\theta, \theta'; \boldsymbol{\psi}_k, \boldsymbol{\psi}_{k'}) &= \mathrm{E}\{s_k(\theta, \boldsymbol{\psi}_k, t) s_{k'}(\theta', \boldsymbol{\psi}_{k'}, t)\}, \\ &= \sigma_{s_k}^2 \gamma_k e^{j\phi_k} \rho_k(\theta, \boldsymbol{\psi}_k) \delta(\theta - \theta') \delta_{kk'}. \end{aligned} \quad (7)$$

where γ_k is the noncircularity rate of the kth source satisfying $0 \leq \gamma_k \leq 1$ and ϕ_k is its noncircularity phase. We assume in this paper that the signals are fully/completely noncircular (i.e. $\gamma_k = 1$). Then, (7) reduces simply to

$$p'_{kk'}(\theta, \theta'; \boldsymbol{\psi}_k, \boldsymbol{\psi}_{k'}) = \sigma_{s_k}^2 e^{j\phi_k} \rho_k(\theta, \boldsymbol{\psi}_k) \delta(\theta - \theta') \delta_{kk'}. \quad (8)$$

We also consider that the sources and noise are uncorrelated, then from (4) and using (6) and (8), the *conjugated* and *unconjugated* covariance matrices of $\boldsymbol{x}(t)$ which are defined, respectively, as $\boldsymbol{R}_{xx} = \mathrm{E}\{\boldsymbol{x}(t)\boldsymbol{x}^H(t)\}$ and $\boldsymbol{R}'_{xx} = \mathrm{E}\{\boldsymbol{x}(t)\boldsymbol{x}^T(t)\}$ have the following expressions:

$$\boldsymbol{R}_{xx} = \sum_{k=1}^{K} \sigma_{s_k}^2 \boldsymbol{R}_s^{(k)}(\boldsymbol{\psi}_k) + \sigma_n^2 \boldsymbol{I}_L, \quad (9)$$

$$\boldsymbol{R}'_{xx} = \sum_{k=1}^{K} \sigma_{s_k}^2 e^{j\phi_k} \boldsymbol{R}_s'^{(k)}(\boldsymbol{\psi}_k), \quad (10)$$

where σ_n^2 is the unknown noise power. Moreover, $\boldsymbol{R}_s^{(k)}(\boldsymbol{\psi}_k)$ and $\boldsymbol{R}_s'^{(k)}(\boldsymbol{\psi}_k)$ represent, respectively, the normalized *conjugated* and *unconjugated* noise-free covariance matrices corresponding to the kth source. They are given by

$$\boldsymbol{R}_s^{(k)}(\boldsymbol{\psi}_k) = \int_{-\pi/2}^{\pi/2} \rho_k(\theta, \boldsymbol{\psi}_k) \boldsymbol{a}(\theta) \boldsymbol{a}^H(\theta) d\theta, \quad (11)$$

$$\boldsymbol{R}_s'^{(k)}(\boldsymbol{\psi}_k) = \int_{-\pi/2}^{\pi/2} \rho_k(\theta, \boldsymbol{\psi}_k) \boldsymbol{a}(\theta) \boldsymbol{a}^T(\theta) d\theta. \quad (12)$$

III. Derivation Of The New DOA Estimation Method

This new method presents an extension of the Efficient Subspace-Based (ESB) method [11] derived for the localization of multiple ID and *circular* sources to *noncircular* sources. In order to take advantage of the signal noncircularity, we define the extended received vector $\widetilde{\boldsymbol{x}}(t) = [\boldsymbol{x}(t), \boldsymbol{x}^*(t)]^T$. Then, the extended covariance matrix can be written as:

$$\boldsymbol{R}_{\widetilde{x}\widetilde{x}} = \mathrm{E}\{\widetilde{\boldsymbol{x}}(t)\widetilde{\boldsymbol{x}}^H(t)\} = \begin{pmatrix} \boldsymbol{R}_{xx} & \boldsymbol{R}'_{xx} \\ \boldsymbol{R}'^*_{xx} & \boldsymbol{R}^*_{xx} \end{pmatrix}, \quad (13)$$

where $\boldsymbol{R}_{xx}$ and $\boldsymbol{R}'_{xx}$ are defined in (9) and (10), respectively. After some algebraic manipulations, we obtain the following expression of the extended covariance matrix:

$$\boldsymbol{R}_{\widetilde{x}\widetilde{x}} = \sum_{k=1}^{K} \int_{-\pi/2}^{\pi/2} \sigma_{s_k}^2 \rho_k(\theta, \boldsymbol{\psi}_k) \widetilde{\boldsymbol{a}}(\theta, \phi_k) \widetilde{\boldsymbol{a}}^H(\theta, \phi_k) d\theta + \sigma_n^2 \boldsymbol{I}_{2L}, (14)$$

in which

$$\widetilde{\boldsymbol{a}}(\theta, \phi_k) = \begin{bmatrix} \boldsymbol{a}(\theta), & \boldsymbol{a}^*(\theta) e^{-j\phi_k} \end{bmatrix}^T. \quad (15)$$

This extended covariance matrix can be also written as:

$$\boldsymbol{R}_{\widetilde{x}\widetilde{x}} = \sum_{k=1}^{K} \sigma_{s_k}^2 \widetilde{\boldsymbol{R}}_s^{(k)}(\boldsymbol{\psi}_k, \phi_k) + \sigma_n^2 \boldsymbol{I}_{2L}, \quad (16)$$

where $\widetilde{\boldsymbol{R}}_s^{(k)}(\boldsymbol{\psi}_k, \phi_k)$ is the normalized extended noise-free covariance matrix corresponding to the kth source and have the following expression:

$$\widetilde{\boldsymbol{R}}_s^{(k)}(\boldsymbol{\psi}_k, \phi_k) = \int_{-\pi/2}^{\pi/2} \rho_k(\theta, \boldsymbol{\psi}_k) \widetilde{\boldsymbol{a}}(\theta, \phi_k) \widetilde{\boldsymbol{a}}^H(\theta, \phi_k) d\theta. \quad (17)$$

$\widetilde{R}_s^{(k)}(\psi_k, \phi_k)$ can be also given by:

$$\widetilde{R}_s^{(k)}(\psi_k, \phi_k) = \begin{pmatrix} R_s^{(k)}(\psi_k) & e^{j\phi_k} R'^{(k)}_s(\psi_k) \\ e^{-j\phi_k} R'^{(k)*}_s(\psi_k) & R_s^{(k)*}(\psi_k) \end{pmatrix}, \quad (18)$$

where $R_s^{(k)}(\psi_k)$ and $R'^{(k)}_s(\psi_k)$ are previously defined in (11) and (12), respectively. Now, to derive the new estimator, we consider the eigendecomposition of $R_{\widetilde{x}\widetilde{x}}$ as follows:

$$R_{\widetilde{x}\widetilde{x}} = \widetilde{U}_s \Sigma \widetilde{U}_s^H + \sigma_n^2 \widetilde{U}_n \widetilde{U}_n^H, \quad (19)$$

where $\widetilde{U}_s = [U_{s1}, U_{s2}]$ and $\widetilde{U}_n = [U_{n1}, U_{n2}]$ denote the partitioned eigenvectors matrices associated with the signal and noise subspaces respectively. Moreover, Σ is a diagonal matrix containing the signal eigenvalues of $R_{\widetilde{x}\widetilde{x}}$. The principle of the signal subspace method in the noncircular ID source case is that the columns of the extended noise-free covariance matrix for the kth ID source are orthogonal with those of the pseudonoise subspace. This means that:

$$\widetilde{U}_n^H \widetilde{R}_s^{(k)}(\psi_k, \phi_k) = \mathbf{0}_{(2L-r) \times 2L}, \quad (20)$$

where r represents the effective dimension of the pseudosignal subspace defined in [4]. We note here that the performance of the method defined in (20) depends on the choice of r. To avoid this problem, we propose, similar to the method in [11], to use the inverse of the extended covariance matrix without any need to the eigendecomposition of $R_{\widetilde{x}\widetilde{x}}$. In fact, inverting (19), we obtain the following matrix

$$R_{\widetilde{x}\widetilde{x}}^{-1} = \widetilde{U}_s \Sigma^{-1} \widetilde{U}_s^H + \frac{1}{\sigma_n^2} \widetilde{U}_n \widetilde{U}_n^H. \quad (21)$$

By multiplying $R_{\widetilde{x}\widetilde{x}}^{-1}$ by $\widetilde{R}_s^{(k)}$, it follows that:

$$R_{\widetilde{x}\widetilde{x}}^{-1} \widetilde{R}_s^{(k)}(\psi_k, \phi_k) = \widetilde{U}_s \Sigma^{-1} \widetilde{U}_s^H \widetilde{R}_s^{(k)}(\psi_k, \phi_k)$$
$$+ \frac{1}{\sigma_n^2} \widetilde{U}_n \widetilde{U}_n^H \widetilde{R}_s^{(k)}(\psi_k, \phi_k). \quad (22)$$

For a high SNR, the signal eigenvalues in Σ are very large and then the different elements of Σ^{-1} are negligible. Consequently, the first term in (22) tend to zero. Moreover, from (20), the second term is very small for $\{\psi_k\}_{k=1}^K$. Consequently, at high SNR, the quantity $\left\| R_{\widetilde{x}\widetilde{x}}^{-1} \widetilde{R}_s^{(k)}(\psi_k, \phi_k) \right\|_{\text{Fro}}$ is very small for the values $\{\psi_k\}_{k=1}^K$. Then, the angular parameters $\{\psi_k\}_{k=1}^K$ can be estimated as the locations of the smallest minima of the following function:

$$f(\psi, \phi) = \left\| \widehat{R}_{\widetilde{x}\widetilde{x}}^{-1} \widetilde{R}_s(\psi, \phi) \right\|_{\text{Fro}}^2 = \text{tr}\{\widetilde{R}_s(\psi, \phi)\widehat{R}_{\widetilde{x}\widetilde{x}}^{-2}\widetilde{R}_s(\psi, \phi)\}. \quad (23)$$

The explicit expression of $\widetilde{R}_s(\psi, \phi)$ depends on the form of the angular distribution of the sources. The most used ones in the literature are the Gaussian, Laplacian and Uniform shapes. Assuming these angular distribution shapes and small angular spreads, it was shown in [5] that the normalized *conjugated* noise-free covariance matrice $R_s(\psi)$ can be written as:

$$R_s(\psi) = a(\bar{\theta})a^H(\bar{\theta}) \odot T(\psi) = \Phi(\bar{\theta})T(\psi)\Phi^H(\bar{\theta}), \quad (24)$$

where

$$\Phi(\bar{\theta}) = \text{diag}\{a(\bar{\theta})\}. \quad (25)$$

Moreover, $T(\psi)$ is a $(L \times L)$ real-valued symmetric Toeplitz matrix. For the sake of brevity, we will give only the expression

of $T(\psi)$ in the case of Gaussian angular distribution and we will consider this form in our simulations. However, the developments given below are also valid for Laplacian and Uniform shapes.

In the case of Gaussian distribution, this matrix has the following expression:

$$[T]_{pl}^{\text{Gauss}}(\psi) = \exp\left(-\frac{1}{2}\left(\frac{2\pi d}{\lambda}(p-l)\sigma\cos(\bar{\theta})\right)^2\right). \quad (26)$$

Moreover, assuming the same angular distributions and small angular spreads, we prove after algebraic manipulations as in [5] that the normalized unconjugated noise-free covariance matrix $R'_s(\psi)$ can be written as follows:

$$R'_s(\psi) = a(\bar{\theta})a^T(\bar{\theta}) \odot T'(\psi) = \Phi(\bar{\theta})T'(\psi)\Phi^T(\bar{\theta}), \quad (27)$$

where $T'(\psi)$ is a $(L \times L)$ real-valued Hankel matrix which has the following expression in the case of Gaussian angular distribution:

$$[T']_{pl}^{\text{Gauss}}(\psi) = \exp\left(-\frac{1}{2}\left(\frac{2\pi d}{\lambda}(p+l-2)\sigma\cos(\bar{\theta})\right)^2\right). \quad (28)$$

Using (24) and (27) in (18), we show after some algebraic manipulations that the normalized extended noise-free covariance matrix $\widetilde{R}_s(\psi, \phi)$ can be written as follows:

$$\widetilde{R}_s(\psi, \phi) = \widetilde{a}(\bar{\theta}, \phi)\widetilde{a}^H(\bar{\theta}, \phi) \odot \widetilde{T}(\psi),$$
$$= \widetilde{\Phi}(\bar{\theta}, \phi)\widetilde{T}(\psi)\widetilde{\Phi}^H(\bar{\theta}, \phi), \quad (29)$$

where

$$\widetilde{\Phi}(\bar{\theta}, \phi) = \text{diag}\{\widetilde{a}(\bar{\theta}, \phi)\}. \quad (30)$$

Moreover, $\widetilde{T}(\psi)$ is given by:

$$\widetilde{T}(\psi) = \begin{pmatrix} T(\psi) & T'(\psi) \\ T'(\psi) & T(\psi) \end{pmatrix}. \quad (31)$$

Inserting (29) in (23), we prove after tedious manipulations (see appendix) that the angular parameters $\psi_k = [\bar{\theta}_k, \sigma_k]^T$ $(k = 1 \ldots K)$ can be estimated as the locations of the smallest minima of the following function:

$$g(\psi) = \Re\{\text{tr}\{\text{diag}\{a(\bar{\theta})\}A(\psi)\text{diag}\{a^H(\bar{\theta})\}R_1\}\}$$
$$- \text{abs}\{\text{tr}\{\text{diag}\{a(\bar{\theta})\}B(\psi)\text{diag}\{a^T(\bar{\theta})\}R_2^*\}\}, \quad (32)$$

where

$$A(\psi) = T^2(\psi) + T'^2(\psi),$$
$$B(\psi) = T(\psi)T'(\psi) + T'(\psi)T(\psi),$$
$$R_1 = \widehat{R}_{\widetilde{x}\widetilde{x}}^{-2}(1:L, 1:L),$$
$$R_2 = \widehat{R}_{\widetilde{x}\widetilde{x}}^{-2}(1:L, L+1:2L).$$

IV. GRAPHICAL REPRESENTATIONS

In this section, we will present some graphical representations to show the performance of our new estimator. This estimator will be compared to the ESB method derived in [11] and the RGC method derived in [10]. Throughout this section, we consider a uniform linear array of 6 sensors separated by a half-wavelength. Moreover, we assume that the emitted signals are complex noncircular Gaussian. The performances of the estimators are obtained by means of 2000 Monte Carlo

simulations by calculating the root mean-square error (RMSE). Furthermore, the number of snapshots used to estimate the sample covariance matrix is 1000. Although our method is not limited to a specific type of the sources' angular distribution, we will consider in our simulations only the case of Gaussian angular distribution for the sake of brevity.

We first consider two uncorrelated noncircular Gaussian sources with the same noncircularity rate ($\gamma_1 = \gamma_2 = 1$) and with phases of noncircularity $\phi_1 = \frac{\pi}{3}$ and $\phi_2 = \frac{\pi}{4}$. The two sources are assumed to be Gaussian distributed (GID). The first one is distributed with central angle $\bar{\theta}_1 = 5°$ and angular spread $\sigma_1 = 1.5°$ while the second one is distributed with central angle $\bar{\theta}_2 = 22°$ and angular spread $\sigma_2 = 3°$. Figs. 1-(a) and 1-(b) present the RMSEs of the estimates of $\bar{\theta}_1$ and σ_1 of our new method versus the SNR for $N = 1000$ snapshots and compared to those of the ESB and the RGC methods.
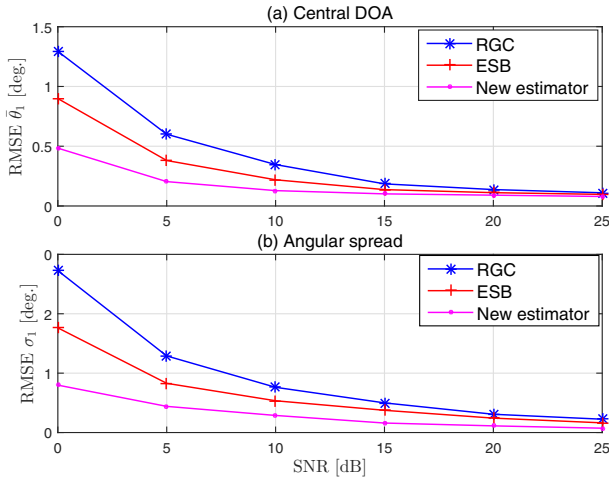

Figure 1. RMSEs of $\bar{\theta}_1$ and σ_1 for the new estimator, ESB and RGC methods versus SNR for $N = 1000$.

We see from these two subfigures that the new proposed method outperform the ESB and the RGC methods in terms of lower RMSE. Moreover, it has a better estimation performance compared with the two other estimators, especially for low SNR values. Moreover, comparing Fig. 1-(a) to Fig. 1-(b), it can be clearly seen that the improvement made by the new estimator is more pronounced for the estimate of the angular spread.

Now, to study the influence of the DOA separation on the performances of the three estimators, we reconsider two noncircular sources with the same angular GID distribution and with the same angular spreads. The first source is kept fixed at 5° while the second source is moved from 13° to 25° with a step of 2°. The SNR is equal to 5 dB. Figs. 2-(a) and 2-(b) display the RMSEs of the estimates of $\bar{\theta}_1$ and σ_1 of the fixed source for the three methods versus the DOA separation $\Delta\theta$ for $N = 1000$ snapshots.

We notice from Figs. 2-(a) and 2-(b) that the performances of the estimators improve when the sources are largely spaced. Moreover, these subfigures show that the new method is statistically more efficient than the ESB and the RGC methods especially for low DOA separation. Finally, Figs. 3-(a) and 3-(b) exhibit the RMSEs of $\bar{\theta}_1$ and σ_1 of new estimator as a function of the noncircularity phase separation $\Delta\phi$ for different DOA separations $\Delta\theta$.

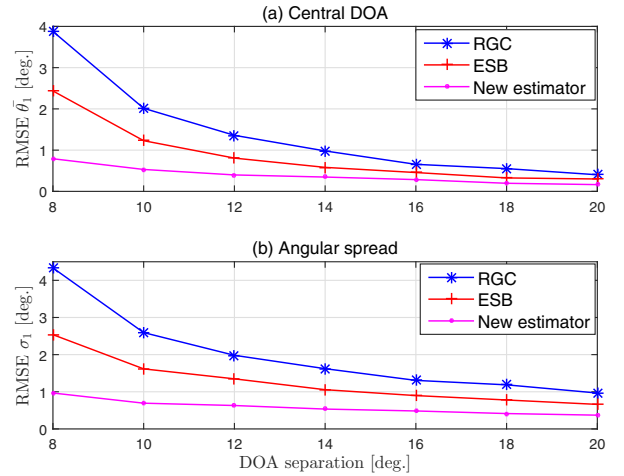We see from these subfigures that the RMSEs of the new extended method depend more on the noncircularity phase

Figure 2. RMSEs of $\bar{\theta}_1$ and σ_1 for the new estimator, ESB and RGC methods versus DOA separation for $N = 1000$, SNR= 5dB.
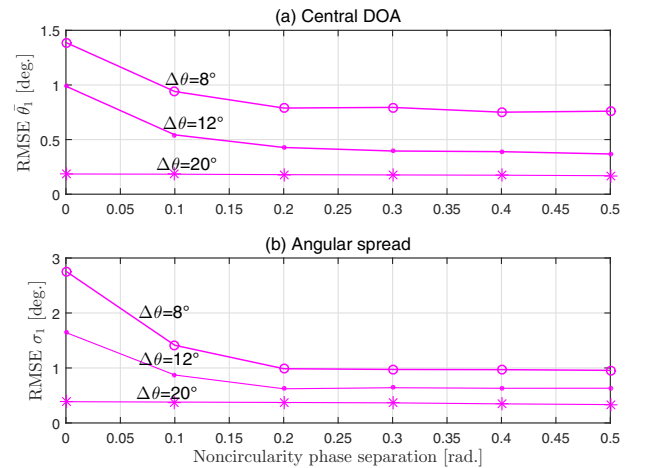

Figure 3. RMSEs of $\bar{\theta}_1$ and σ_1 for the new estimator versus noncircularity phase separation $\Delta\phi$ for different DOA separations $\Delta\theta$ for $N = 1000$.

separation $\Delta\phi$ when the DOA separation $\Delta\theta = 8°$ while they are almost insensitive to $\Delta\phi$ when $\Delta\theta = 20°$. We can then conclude that the sensitivity of the performance of the new method on the noncircularity phase separation $\Delta\phi$ is more prominent for low DOA separations.

V. CONCLUSION

In this paper, we developed for the first time a new method for estimating the angular parameters assuming noncircular and incoherently distributed signals. This method extends the well known ESB approach to noncircular signals. The new estimator was compared to the most recent state-of-the-art techniques on the subject of DOA estimation of multiple ID sources which are the ESB and the RGC estimators. We proved that our newly proposed method outperforms the two other methods in terms of lower RMSE. This improvement is more prominent for low SNR levels. Moreover, we showed that the new estimator is statistically more efficient than the ESB and RGC methods especially for the more challenging scenario of low DOA separation. Finally, when the sources are largely spaced, the performance of the new estimator holds almost the same regardless of the noncircularity phase separation $\Delta\phi$.

APPENDIX - DERIVATION OF $g(\psi)$

We have from (23):

$$f(\psi, \phi) = \text{tr}(\widetilde{\boldsymbol{R}}_s(\psi, \phi)\hat{\boldsymbol{R}}_{\tilde{x}\tilde{x}}^{-2}\widetilde{\boldsymbol{R}}_s(\psi, \phi)). \qquad (33)$$

We insert (29) in (33) and we use the following identity:

$$\widetilde{\boldsymbol{\Phi}}^H(\bar{\theta}, \phi)\widetilde{\boldsymbol{\Phi}}(\bar{\theta}, \phi) = \boldsymbol{I}_{2L}, \qquad (34)$$

we obtain the following expression of $f(\psi, \phi)$:

$$f(\psi, \phi) = \text{tr}\left(\widetilde{\boldsymbol{\Phi}}(\bar{\theta}, \phi)\widetilde{\boldsymbol{T}}^2(\psi)\widetilde{\boldsymbol{\Phi}}^H(\bar{\theta}, \phi)\hat{\boldsymbol{R}}_{\tilde{x}\tilde{x}}^{-2}\right). \qquad (35)$$

Otherwise, we have:

$$\widetilde{\boldsymbol{\Phi}}(\bar{\theta}, \phi) = \text{diag}(\widetilde{\boldsymbol{a}}(\bar{\theta}, \phi)),$$
$$= \begin{pmatrix} \text{diag}(\boldsymbol{a}(\bar{\theta})) & \boldsymbol{0}_{L\times L} \\ \boldsymbol{0}_{L\times L} & e^{-j\phi}\text{diag}(\boldsymbol{a}^*(\bar{\theta})) \end{pmatrix}. \qquad (36)$$

Moreover, we show from (31) that:

$$\widetilde{\boldsymbol{T}}^2(\psi) = \begin{pmatrix} \boldsymbol{A}(\psi) & \boldsymbol{B}(\psi) \\ \boldsymbol{B}(\psi) & \boldsymbol{A}(\psi) \end{pmatrix}, \qquad (37)$$

where

$$\boldsymbol{A}(\psi) = \boldsymbol{T}^2(\psi) + \boldsymbol{T'}^2(\psi),$$
$$\boldsymbol{B}(\psi) = \boldsymbol{T}(\psi)\boldsymbol{T'}(\psi) + \boldsymbol{T'}(\psi)\boldsymbol{T}(\psi).$$

Now, from (19), $\hat{\boldsymbol{R}}_{\tilde{x}\tilde{x}}^{-2}$ can be eigendecomposed as:

$$\hat{\boldsymbol{R}}_{\tilde{x}\tilde{x}}^{-2} = \begin{pmatrix} \hat{\boldsymbol{U}}_{s1} \\ \hat{\boldsymbol{U}}_{s2} \end{pmatrix}\hat{\boldsymbol{\Sigma}}^{-2}\begin{pmatrix} \hat{\boldsymbol{U}}_{s1}^H & \hat{\boldsymbol{U}}_{s2}^H \end{pmatrix} + \begin{pmatrix} \hat{\boldsymbol{U}}_{n1} \\ \hat{\boldsymbol{U}}_{n2} \end{pmatrix}\hat{\boldsymbol{\Sigma}}_n^{-2}\begin{pmatrix} \hat{\boldsymbol{U}}_{n1}^H & \hat{\boldsymbol{U}}_{n2}^H \end{pmatrix} (38)$$

Otherwise, we have from [12] that $\hat{\boldsymbol{U}}_{s2} = \hat{\boldsymbol{U}}_{s1}^*\Delta_s$ and $\hat{\boldsymbol{U}}_{n2} = \hat{\boldsymbol{U}}_{n1}^*\Delta_n$ with Δ_s and Δ_n are diagonal matrices whose diagonals are composed of unit modulus complex terms. Using these identities in (38), we show that $\hat{\boldsymbol{R}}_{\tilde{x}\tilde{x}}^{-2}$ can be written as:

$$\hat{\boldsymbol{R}}_{\tilde{x}\tilde{x}}^{-2} = \begin{pmatrix} \boldsymbol{R}_1 & \boldsymbol{R}_2 \\ \boldsymbol{R}_2^* & \boldsymbol{R}_1^* \end{pmatrix}, \qquad (39)$$

where

$$\boldsymbol{R}_1 = \hat{\boldsymbol{U}}_{s1}\hat{\boldsymbol{\Sigma}}^{-2}\hat{\boldsymbol{U}}_{s1}^H + \hat{\boldsymbol{U}}_{n1}\hat{\boldsymbol{\Sigma}}_n\hat{\boldsymbol{U}}_{n1}^H,$$
$$\boldsymbol{R}_2 = \hat{\boldsymbol{U}}_{s1}\hat{\boldsymbol{\Sigma}}^{-2}\Delta_s^*\hat{\boldsymbol{U}}_{s1}^T + \hat{\boldsymbol{U}}_{n1}\hat{\boldsymbol{\Sigma}}_n\Delta_n^*\hat{\boldsymbol{U}}_{n1}^T.$$

Substituting (36), (37) and (39) in (35), we obtain after some algebraic manipulations the following expression of $f(\psi, \phi)$:

$$f(\psi, \phi) = 2\Re\{\text{tr}(\text{diag}(\boldsymbol{a}(\bar{\theta}))\boldsymbol{A}(\psi)\text{diag}(\boldsymbol{a}^H(\bar{\theta}))\boldsymbol{R}_1)\}$$
$$+ 2\Re\{e^{j\phi}\text{tr}(\text{diag}(\boldsymbol{a}(\bar{\theta}))\boldsymbol{B}(\psi)\text{diag}(\boldsymbol{a}^T(\bar{\theta}))\boldsymbol{R}_2^*)\}. (40)$$

We minimize the expression of $f(\psi, \phi)$ in (40) with respect to ϕ. We show that this function is minimum for:

$$\phi_{\min} = \pi - \text{angle}(\text{tr}(\text{diag}(\boldsymbol{a}(\bar{\theta}))\boldsymbol{B}(\psi)\text{diag}(\boldsymbol{a}^T(\bar{\theta}))\boldsymbol{R}_2^*)).$$

Consequently, minimizing (35) with respect to ϕ and ψ is equivalent to minimize the function $g(\psi)$ given in (32) with respect to ψ.

REFERENCES

[1] P. Stoica and A. Nehorai, "MUSIC, Maximum Likelihood, and Cramér-Rao Bound: Further Results and Comparisons," *IEEE Trans. Acoust., Speech, Sig. Process.*, vol. 38, pp. 2140-2150, Dec. 1990.

[2] R. Roy, T. Kailath, and A.B. Gershman, "ESPRIT, Estimation of Signal Parameters via Rotational Invariance Techniques," *IEEE Trans. Acoust., Speech, Sig. Process.*, vol. 37, pp. 984-995, July 1989.

[3] F. Haddadi, M.M. Nayebi, and M.R. Aref, "Direction-of-Arrival Estimation for emporally Correlated Narrowband Signals," *IEEE Trans. Sig. Process.,* vol. 57, pp. 600-609, Apr. 2009.

[4] Y. Meng, P. Stoica, and K. M.Wong, "Estimation of the directions of arrival of spatially dispersed signals in array processing," *Proc. Inst. Elect. Eng.-Radar, Sonar Navigat.*, vol. 143, pp. 1-9, Feb. 1996.

[5] M. Bengtsson, "Antenna array signal processing for high rank models," *Ph.D. dissertation, Signals, Sensors, Syst. Dept., Royal Institute of Technology, Stockholm, Sweden*, 1999.

[6] S. Shahbazpanahi, A.B. Gershman, Z.-Q. Luo, and K.M. Wong , "Robust adaptive beamforming for general-rank signal models," *IEEE Trans. Signal Process.*, vol. 51, no. 9, pp. 2257-2269, Sept. 2003.

[7] A. Hassanien, S. Shahbazpanahi, and A. B. Gershman, "A generalized Capon estimator for localization of multiple spread sources," *IEEE Trans. Signal Process.*, vol. 52, no. 1, pp. 280-283, Jan. 2004.

[8] A. Zoubir, Y. Wang, and P. Chargé, "A modified COMET-EXIP method for estimating a scattered source," *Elsevier Signal Process. J.*, vol. 86, pp. 733-743, Feb. 2006.

[9] Sh. Shahbazpanahi, Sh. Valaee, and A. B. Gershman, "A Covariance Fitting Approach to Parametric Localization of Multiple Incoherently Distributed Sources,"*IEEE Trans. sig. Process.,* vol. 52, no. 3, March 2004.

[10] A. Zoubir, and Y. Wang, "Robust generalised Capon algorithm for estimating the angular parameters of multiple incoherently distributed sources," *IET Signal Process.,* vol. 2, no. 2, pp. 163-168, Dec. 2007.

[11] A. Zoubir, Y. Wang, and P. Chargé, "Efficient Subspace-Based Estimator for Localization of Multiple Incoherently Distributed Sources," *IEEE Trans. sig. Process.,* vol. 56, no. 2, pp. 532-542, Feb. 2008

[12] H. Abeida and J.P. Delmas, "MUSIC-Like Estimation of Direction of Arrival for Noncircular Sources," *IEEE Trans. Sig. Process.,* vol. 54, pp. 2678-2689, July 2006.

[13] S. Ben Hassen, F. Bellili, A. Samet and S. Affes, "DOA Estimation of Temporally and Spatially Correlated Narrowband Noncircular Sources in Spatially Correlated White Noise," *IEEE Trans. Sig. Process.,* vol. 59, pp. 4108-4121, Sept. 2011.

[14] M. Zhong, Z. Fan, "Direction-of-arrival estimation for noncircular signals," *Int. Conf. on Computer, Networks and Communication Engineering (ICCNCE), Beijing, China*, 634-637, May. 2013.